# Dielectric Screening Model for Lattice Vibrations of Diamond-Structure Crystals*†

RICHARD M. MARTIN‡§
*The James Franck Institute and Department of Physics, The University of Chicago, Chicago, Illinois 60637*
(Received 4 April, 1969)

The phonon dispersion curves of Si are calculated from the dielectric screening theory using approximations based on Phillips's bond-charge model for covalent crystals. The off-diagonal ($K \neq K'$) elements of the inverse dielectric function $\epsilon^{-1}(\mathbf{q}+\mathbf{K}, \mathbf{q}+\mathbf{K}')$ are essential in the calculation for a nonmetal; here their effect is approximated by the interactions involving the bond charges. The diagonal part is calculated within the pseudopotential framework. One adjustable parameter, which affects only the LA modes, is used. The results are generally in good agreement with experiment (of order 10% except for the low acoustic modes for which the maximum error is 36%). The calculation suggests a two-parameter model for the forces, which can readily be applied to all crystals with the diamond structure. In agreement with the assumptions of the bond-charge model, it is found that the major deviations from homology of the dispersion curves of the different elements are explained by the decreasing importance of the bond-charge forces as the dielectric constant increases.

## I. INTRODUCTION

THEORETICAL analysis of atomic vibrations in crystals has usually been undertaken on two distinct levels: fitting empirical vibration frequencies or direct derivation from models of the electronic structure of the undistorted crystal. In the former category are the strictly phenomenological Born–von Karman force constant models[1,2] and other parametrized models for the forces. This approach satisfactorily explains the forces only if all parameters have clear physical meanings in terms of the electronic properties and are well determined by the data. In practice, the derivation of lattice vibration frequencies, i.e., phonon dispersion curves, from the electronic structure has been limited almost exclusively to simple metals. Calculations have been carried out successfully for many nearly free-electron (NFE) metals (see, for example, the review by Joshi and Rajagopal[3]). In insulators, however, the response of the electrons to the ion displacements is much less well understood, and only a few attempts[4–8] to derive dispersion curves have been made.

The purpose of this paper is to present and to apply a method for calculation of the dispersion curves which can be used for insulators. The present method is based on the general microscopic theory of lattice dynamics given by Pick, Cohen, and Martin[9] (henceforth referred to as I) which is applicable to any material and thus, in principle, bridges the gap between metals and insulators. In I, several important features of the microscopic theory as applied to insulators have been derived. The most important results are summarized here in Sec. II.

The detailed approximations needed to carry out the calculations are given in Secs. IV–VI for covalent crystals of the diamond structure, and are based on Phillips's bond-charge model[10] of the charge density in covalent materials. The results of the calculations are presented for the case of silicon. Many of the results of the present paper have been previously reported in a short communication.[11]

Silicon is chosen for this first application of the general theory to insulators for several reasons. Most important is that over a wide range of energy of order $E_F \sim 12$ eV, the electronic structure of Si is very NFE-like,[12–14] so that we expect minimum deviations from the calculational methods which are well established for NFE metals. Second, Phillips has given a particularly simple model[10] of the charge density. Finally, the phonon dispersion curves for Si have been measured accurately for the principal symmetry directions by inelastic neutron scattering.[15,16] All methods used here should apply

* Supported in part by the U. S. Office of Naval Research, the National Aeronautics and Space Administration, and the Advanced Research Projects Agency.
† Submitted in partial fulfillment of the degree of Doctor of Philosophy at the University of Chicago.
‡ National Science Foundation Predoctoral Fellow.
§ Present address: Bell Telephone Laboratories, Murray Hill, N. J. 07974.
[1] M. Born and K. Huang, *Dynamical Theory of Crystal Lattices* (Oxford University Press, London, 1954).
[2] M. Born and T. von Karman, Z. Physik **13**, 297 (1912).
[3] S. K. Joshi and A. K. Rajagopal, in *Solid State Physics*, edited by F. Seitz and D. Turnbull (Academic Press Inc., New York, 1969), Vol. 22, p. 159. In the general discussion, no restriction to the Born-Oppenheimer approximation is made.
[4] S. O. Lundquist, Arkiv Fysik **12**, 263 (1957).
[5] K. B. Tolpygo, Fiz. Tverd. Tela **3**, 943 (1961) [English transl.: Soviet Phys.—Solid State **3**, 685 (1961)].
[6] J. A. Young and A. A. Maradudin, Bull. Am. Phys. Soc. **12**, 690 (1967).
[7] B. Gliss and H. Biltz, Phys. Rev. Letters **21**, 884 (1968).
[8] A. A. Maradudin (unpublished).
[9] R. M. Pick, M. H. Cohen, and R. M. Martin (to be published). A preliminary report of this work may be found in *Inelastic Neutron Scattering* (International Atomic Energy Agency, Vienna, 1968), Vol. I, p. 119.
[10] J. C. Phillips, Phys. Rev. **166**, 832 (1968); *Covalent Bonding in Crystals and Molecules* (University of Chicago Press, Chicago, to be published).
[11] R. M. Martin, Phys. Rev. Letters **21**, 536 (1968).
[12] F. Herman, Rev. Mod. Phys. **30**, 102 (1968).
[13] W. A. Harrison, Physica **31**, 1692 (1965).
[14] V. Heine and R. O. Jones (unpublished).
[15] G. Dolling, *Inelastic Scattering of Neutrons in Solids and Liquids* (International Atomic Energy Agency, Vienna, 1963), Vol. II, p. 37.
[16] H. Palevsky, D. J. Hughes, W. Kley, and E. Tunkelo, Phys. Rev. Letters **2**, 258 (1959).

equally well to Ge and grey Sn (with the exception of any effects of the vanishing band gap[17] in grey Sn); however, the dispersion curves for Ge [18] have not been measured so completely as those for Si, and similar experiments on grey Sn [19] had not been carried out at the start of this work. In the case of diamond the dispersion curves[20] are known in detail, but the application of the theory would be more difficult because of the larger gaps in the energy bands (see Sec. V).

There have been many parametrized fittings[15,20–25] of the dispersion curves of the diamond-structure crystals. Most notable for this paper are the shell-model methods[5,15,20,22,23,26] and the valence force field approach.[24,25] The shell model has been shown by Tolpygo[5] to be formally equivalent to the forces derived from the distortions of the electronic bonding orbitals, so the parameters in the shell model have definite interpretations in a quantum-mechanical model. However, there remains the necessity of employing many parameters to fit the dispersion curves, so that in practice it is difficult to interpret the forces, e.g., to understand the deviations from homology among the dispersion curves of the group-IV elements. The valence force field model is of note because it affords a particularly lucid picture of the forces in a covalently bonded material, and because in some cases, the necessary force constants can be transferred from crystal to molecule (e.g., diamond to some hydrocarbons[24,25]).

In Sec. VII, the calculated real space force constants for Si are reported and the contributions of the various forces to the frequencies are determined. The results suggest a two-parameter *simple bond-charge* model which is applied to all the diamond-structure crystals in Sec. VIII. The major differences in the shapes of the dispersion curves of these elements are understood quantitatively in this model simply in terms of the relative importance of the Coulombic forces as opposed to the short-range non-Coulombic forces.

## II. GENERAL MICROSCOPIC THEORY AND ACOUSTIC SUM RULE

In the Born–von Karman theory[1,2] of the vibrations of nuclei in solids, the equations of motion of the displacements of the nuclei from their equilibrium positions are those of coupled harmonic oscillators. We consider only the case of a perfect crystal in which the nuclei may be labeled by the unit cell index $l$ and the index $s=1\cdots n$ of the nuclei in the unit cell. Let us denote equilibrium positions of the nuclei by $\mathbf{R}_{sl}=\mathbf{R}_s+\mathbf{R}_l$. The Born–von Karman force constant coupling nuclei $s$, $l$ and $s'$, $l'$ is

$$C_{sl's'l'}{}^{\alpha\beta}=C_{ss'}{}^{\alpha\beta}(l-l'), \tag{2.1}$$

where $\alpha$, $\beta$ are Cartesian components, and (2.1) follows from the translational symmetry of the crystal. The Born–von Karman periodic boundary conditions[1,2] allow the immediate diagonalization of the force constant matrix (2.1) in the $l,l'$ indices. The resulting normal-mode displacements $u_{sl}{}^{\alpha}(\mathbf{q},\lambda)$ of the nuclei from the equilibrium positions are infinite waves

$$u_{sl}{}^{\alpha}(\mathbf{q},\lambda)=u_s{}^{\alpha}(\mathbf{q},\lambda)e^{i\mathbf{q}\cdot\mathbf{R}_{sl}}+\text{c.c.}, \tag{2.2}$$

where $\mathbf{q}$ is the wave vector and $\lambda=1,\cdots,3n$ is the normal-mode index. For each wave vector $\mathbf{q}$, the squares of the normal-mode vibration frequencies $\omega_\lambda{}^2(\mathbf{q})$ are the eigenvalues of the $3n\times 3n$ dynamical matrix

$$D_{ss'}{}^{\alpha\beta}(\mathbf{q})=(M_sM_{s'})^{-1/2}\sum_l C_{ss'}{}^{\alpha\beta}(l)e^{i\mathbf{q}\cdot(\mathbf{R}_{s'0}-\mathbf{R}_{sl})}, \tag{2.3}$$

where $M_s$ is the mass of a nucleus of type $s$.

Within the Born-Oppenheimer approximation,[1,27] in which the nuclear and electronic motions are assumed to be decoupled, the dynamical matrix has been derived from the electronic states of the crystal. This approach is here termed the microscopic theory of lattice vibrations. The derivation has been given by several authors,[3,9,28–33] the most recent and most concise derivation being that of Pick, Cohen, and Martin.[9] The Born-Oppenheimer approximation is valid in any insulator,[1,27] and its breakdown is quantitatively unimportant in the lattice dynamics of ordinary metals.[34] Thus, it is appropriate for any application discussed in this paper.

In I, the dynamical matrix has been derived in the most general form, treating all the electrons on the same

[17] S. Groves and W. Paul, Phys. Rev. Letters **11**, 194 (1963); L. Liu and D. Brust, *ibid.* **20**, 651 (1968).
[18] B. N. Brockhouse and P. K. Iyengar, Phys. Rev. **111**, 747 (1958); B. N. Brockhouse and B. A. Dasannacharya, Solid State Commun. **1**, 205 (1958).
[19] D. L. Price and J. M. Rowe (private communication).
[20] J. L. Warren, J. L. Yarnell, G. Dolling, and R. A. Cowley, Phys. Rev. **158**, 805 (1967).
[21] F Herman, J. Phys. Chem. Solids **8**, 405 (1959); N. K. Pope, *Lattice Dynamics*, edited by R. F. Wallis (Pergamon Press, Ltd., Oxford, 1965), p. 147.
[22] W. Cochran, Proc. Roy. Soc. (London) **A253**, 260 (1959).
[23] T. I. Kucher and V. V. Nechiporuk, Fiz. Tverd. Tela **8**, 317 (1966) [English transl.: Soviet Phys.—Solid State **8**, 261 (1966)], and other references therein.
[24] M. J. P. Musgrave and J. A. Pople, Proc. Roy. Soc. (London) **A268**, 474 (1962).
[25] H. L. McMurray, A. W. Solbrig, Jr., J. K. Boyter, and C. Noble, J. Phys. Chem. Solids **28**, 2359 (1967). Similar calculations have been carried out for Si; A. W. Solbrig, Jr. (private communication).
[26] R. A. Cowley, Proc. Roy. Soc. (London) **A268**, 109 (1962).
[27] M. Born and R. Oppenheimer, Ann. Physik **84**, 457 (1927).
[28] T. Toya, J. Res. Inst. Catalysis, Hokkaido Univ. **6**, 183 (1958).
[29] G. Baym, Ann. Phys. (N.Y.) **14**, 1 (1961).
[30] L. J. Sham, Proc. Roy. Soc. (London) **A283**, 33 (1965); thesis, Cambridge University, 1963 (unpublished).
[31] S. H. Vosko, R. Taylor, and G. H. Keech, Can. J. Phys. **43**, 1187 (1965).
[32] W. A. Harrison, *Pseudopotentials in the Theory of Metals* (W. A. Benjamin, Inc., New York, 1966).
[33] P. N. Keating, Phys. Rev. **175**, 1171 (1968) [who, along with Joshi and Rajagopal (Ref. 3), did not restrict himself to Born-Oppenheimer approximation].
[34] G. V. Chester, Advan. Phys. **10**, 357 (1961).

footing. Here we assume (1) that the closed-shell ion cores move rigidly with the nuclei, (2) the cores do not overlap, (3) the bare-ion–core pseudopotential[35] as seen by a valence electron is a local potential $v_s(|\mathbf{r}-\mathbf{R}_{sl}|)$, and (4) the inverse dielectric screening function of the electrons is determined primarily by the smooth part of the wave functions, i.e., the pseudo-wave-functions. The pseudopotential method is necessary because the approximations for the valence electrons made in the present work are appropriate only for the smooth part of the electronic wave functions.

The results of I for electrons interacting with bare nuclei can be taken over to the present pseudopotential interaction. The microscopic formula for the dynamical matrix becomes

$$D_{ss'}{}^{\alpha\beta}(\mathbf{q})=(M_sM_{s'})^{-1/2}[\tilde{C}_{ss'}{}^{\alpha\beta}(\mathbf{q})-\delta_{ss'}\sum_{s''}\tilde{C}_{ss''}{}^{\alpha\beta}(0)], \tag{2.4}$$

where

$$\tilde{C}_{ss'}{}^{\alpha\beta}(\mathbf{q})=(\Omega/4\pi e^2)\sum_{\mathbf{K},\mathbf{K}'}(\mathbf{q}+\mathbf{K})^{\alpha}v_s(|\mathbf{q}+\mathbf{K}|)\times e^{i\mathbf{K}\cdot\mathbf{R}_s}|\mathbf{q}+\mathbf{K}|^2\epsilon^{-1}(\mathbf{q}+\mathbf{K},\mathbf{q}+\mathbf{K}')(\mathbf{q}+\mathbf{K}')^{\beta}\times v_{s'}(|\mathbf{q}+\mathbf{K}'|)e^{-i\mathbf{K}'\cdot\mathbf{R}_{s'}}. \tag{2.5}$$

The matrix $\tilde{C}_{ss'}{}^{\alpha\beta}(\mathbf{q})$ will also be referred to as the dynamical matrix when there is no danger of confusion. The form of the dynamical matrix in (2.4) follows from the translation invariance of the system (see I). In Eq. (2.5), $\Omega$ is the volume of the unit cell, $\mathbf{K}$ and $\mathbf{K}'$ are reciprocal-lattice vectors, $v_s(|\mathbf{q}+\mathbf{K}|)$ is the Fourier transform of the bare-ion–core pseudopotential

$$v_s(|\mathbf{q}+\mathbf{K}|)=\frac{1}{\Omega}\int v_s(|\mathbf{r}|)e^{i(\mathbf{q}+\mathbf{K})\cdot\mathbf{r}}d^3r,$$

and $\epsilon^{-1}(\mathbf{q}+\mathbf{K},\mathbf{q}+\mathbf{K}')$ is the inverse dielectric function for the valence electrons. If $\epsilon^{-1}$ is defined only in terms of the pseudo-wave-functions, then in addition to (2.5), there are orthogonalization charge corrections.[36] These orthogonalization terms are omitted in the present work since they are very small for a small ion core, as is the case in Si. The sum in (2.5) must, of course, be evaluated by an Ewald transformation.[1,37]

Let us here note the long-wavelength properties of $\epsilon^{-1}(\mathbf{q},\mathbf{q})$ and $v_s(|\mathbf{q}|)$, which are needed later. Adler[38] and Wiser[39] have shown that

$$\lim_{q\to0}\epsilon^{-1}(\mathbf{q},\mathbf{q})=1/\epsilon_0, \tag{2.6}$$

where $\epsilon_0$ is the low-frequency "optical" dielectric constant. (Only cubic crystals are considered here.) The bare-ion–core potential has the form, as $q\to0$,

$$v_s(q)\to-(4\pi e^2/\Omega)(Z_s/q^2), \tag{2.7}$$

where $Z_s$ is the ion-core charge.

In I, it was shown that for any insulator the microscopic theory recaptures completely the phenomenological theory of ionic crystals.[1,40,41] That is, the dynamical matrix can be written

$$\tilde{C}_{ss'}{}^{\alpha\beta}(\mathbf{q})=\tilde{C}_{ss'}{}^{\alpha\beta}(\mathbf{q},1)+\tilde{C}_{ss'}{}^{\alpha\beta}(\mathbf{q},2), \tag{2.8}$$

where $\tilde{C}_{ss'}{}^{\alpha\beta}(\mathbf{q},1)$ is always an analytic function of $\mathbf{q}$, and in a cubic crystal it can be shown that $\tilde{C}_{ss'}{}^{\alpha\beta}(q,2)$ has the limiting behavior

$$\tilde{C}_{ss'}{}^{\alpha\beta}(\mathbf{q},2)\xrightarrow[q\to0]{}\frac{4\pi e^2}{\Omega}\frac{Z_s{}^*Z_{s'}{}^*}{\epsilon_0}\frac{q^{\alpha}q^{\beta}}{q^2},\quad\text{as } q\to0. \tag{2.9}$$

The microscopic formula for the effective charge $Z_s{}^*$ ("dynamic" or "Born" definition[40–42]) is[9]

$$Z_s{}^*=-\frac{\Omega}{4\pi e^2}\lim_{q\to0}\sum_{\mathbf{K}}\frac{\epsilon^{-1}(\mathbf{q},\mathbf{q}+\mathbf{K})}{\epsilon^{-1}(\mathbf{q},\mathbf{q})}\mathbf{q}\cdot(\mathbf{q}+\mathbf{K})\times v_s(|\mathbf{q}+\mathbf{K}|)e^{-i\mathbf{K}\cdot\mathbf{R}_s}. \tag{2.10}$$

The result of primary importance for non-ionic crystals is found by examining the long-wavelength acoustic modes. The requirement that all acoustic-mode frequencies vanish as $q\to0$ may easily be shown to imply a "charge neutrality" condition on the effective charges

$$\sum_s Z_s{}^*=0. \tag{2.11}$$

The condition (2.11) has been recognized in the phenomenological theories[1,40,42]; now it assumes a new importance because inserting (2.10) into (2.11) yields a condition on $\epsilon^{-1}$ in the long-wavelength limit:

$$\lim_{q\to0}\sum_{s,\mathbf{K}}\epsilon^{-1}(\mathbf{q},\mathbf{q}+\mathbf{K})\mathbf{q}\cdot(\mathbf{q}+\mathbf{K})v_s(|\mathbf{q}+\mathbf{K}|)e^{-i\mathbf{K}\cdot\mathbf{R}_s}=0. \tag{2.12}$$

The condition (2.12) was termed the *acoustic sum rule* in I.

The acoustic sum rule is a nontrivial requirement on the inverse dielectric function of any insulator because in general every term in the sum in (2.12) is finite. In particular, Eqs. (2.6) and (2.7) show that the $\mathbf{K}=0$ term in the sum in (2.12) is always nonzero for some direction of $\mathbf{q}$. The sum rule (2.12) can be satisfied only if there is a cancellation between the diagonal ($\mathbf{K}=\mathbf{K}'$) and the off-diagonal ($\mathbf{K}\neq\mathbf{K}'$) terms of $\epsilon^{-1}(\mathbf{q}+\mathbf{K},\mathbf{q}+\mathbf{K}')$.

[35] J. C. Phillips and L. Kleinman, Phys. Rev. **116**, 287 (1959); M. H. Cohen and V. Heine, *ibid.* **122**, 1821 (1961).
[36] W. A. Harrison, Phys. Rev. **129**, 2503 (1963).
[37] P. P. Ewald, Ann. Physik **64**, 235 (1921); E. W. Kellerman, Phil. Trans. Roy. Soc. **238**, 513 (1940).
[38] S. Adler, Phys. Rev. **126**, 413 (1962).
[39] N. Wiser, Phys. Rev. **129**, 62 (1963).
[40] W. Cochran and R. A. Cowley, J. Phys. Chem. Solids **23**, 447 (1962).
[41] M. Born and M. Goppert-Meyer, in *Handbuch der Physik*, edited by S. Flügge (Springer-Verlag, Berlin, 1933), Vol. 24, p. 638.
[42] E. Burstein, *Lattice Dynamics*, edited by R. F. Wallis (Pergamon Press, Ltd., Oxford, 1965), p. 315.

Therefore, it follows that in any insulator, ionic or non-ionic, the dielectric function $\epsilon(\mathbf{q}+\mathbf{K}, \mathbf{q}+\mathbf{K}')$ and its inverse are *never* diagonal matrices.

The acoustic sum rule (2.12) is not a necessary condition for a metal, because the part of the dynamical matrix $\bar{C}_{ss'}{}^{\alpha\beta}(\mathbf{q},2)$ always vanishes as $q \to 0$, owing to the presence of the factor of $1/\epsilon_0$ in (2.9). Thus, the acoustic sum rule places no restriction on the dielectric function for a metal; in particular, a diagonal dielectric function is not excluded for a metal.

The acoustic sum rule points to a crucial factor in the tremendous computational differences between metals and nonmetals. For a metal, any dielectric function having the characteristic form for a metal[9,38,39] at small $q$ can be used. For an insulator, on the other hand, the entire dielectric function matrix must be determined accurately merely to ensure the acoustic mode frequencies all approach zero at long wavelength. Moreover, the acoustic sum rule (2.12) is a relation between the bare-ion–core potential and the inverse dielectric function which is derived from the exact electronic states of the crystal. That (2.12) is satisfied can be guaranteed only if a completely self-consistent band-structure calculation is carried out. Thus, from the acoustic sum rule, we see the difficulty in any calculation of the dynamical matrix for an insulator solely from the electronic structure.

In the following sections, we approximate the important contributions of $\epsilon^{-1}$ to the dynamical matrix, rather than attempting to calculate $\epsilon^{-1}$ from the electronic states. The acoustic sum rule is *utilized* to extract information about the off-diagonal terms, and thus it is automatically satisfied. As the first step, we examine the previous calculations which have been carried out with much success for many NFE metals.

## III. FREE-ELECTRON MODEL

For a metal the acoustic sum rule places no restriction on the dielectric function matrix. Wiser[39] has explicitly shown that all the off-diagonal elements of the $\epsilon$ matrix (calculated from the pseudo-wave-functions) are small compared to the diagonal elements in any NFE metal. Therefore, in the pseudopotential calculation of the dynamical matrix for the NFE metals, it is a good approximation to neglect all off-diagonal elements of $\epsilon^{-1}$. Specifically, the diagonal part of the $\epsilon^{-1}$ matrix is taken to be that given by the free-electron (FE) function with exchange.[43–45] The FE approximation has been applied to the calculation of phonon dispersion curves in many NFE metals (see, e.g., Refs. 31, 32, and 46) with results generally in good agreement with experiment.

Despite the fact that silicon is a semiconductor, it is informative to calculate its dispersion curves in the FE approximation. Indeed, Si is NFE-like in many respects. The dielectric constant $\epsilon_0$ in Si is 12,[47] which is much greater than 1, suggesting that the approximation of metallic behavior, $\epsilon_0 = \infty$, is not bad. Examination of the band structure[12] shows that it is quite FE-like with the band gaps appearing as perturbations. The valence charge density has been computed by Harrison[13] in the FE approximation with results close to the charge density measured by x-ray diffraction.[48] Finally, the cohesive energy is well accounted for by treating it as a metal.[49] Therefore, we expect some aspects of the FE approximation to apply to Si.

The phonon dispersion curves have been calculated for the principal symmetry directions [100], [110], and [111]. The FE dielectric function for the Si valence electron density, including the Hubbard-Sham exchange correction,[43] was employed along with a model potential for the ion core, which is described in Sec. V (where it is labeled the MHA potential). The results are shown as the solid curves in Fig. 1, where they are compared with the experimental frequencies.[15,16]

The most prominent feature of the calculated dispersion curves is that all transverse acoustic (TA) modes have imaginary frequencies, i.e., the crystal is energetically unstable against shear distortions of any wave vector. This instability is not unexpected. The very existence of the loosely packed tetrahedrally coordinated diamond structure has long been considered to be a manifestation of the directed $sp^3$ covalent bonding in a molecular orbital picture, the anisotropy of which is completely omitted in the FE approximation. Born and co-workers[50] have shown by many examples that for central forces only, the more loosely packed a crystal structure, the greater its tendency toward instability. The instability is averted by the increased proportion of noncentral forces. Specifically, Born[51] showed that the diamond lattice is unstable against shear in the presence of central nearest-neighbor forces only. However, any diagonal $\epsilon^{-1}$ gives rise to purely central forces, and in the FE approximation, the forces are almost entirely first-neighbor. Thus, the FE approximation falls in the category of Born's simple model and cannot stabilize the lattice.[52]

[43] Exchange is incorporated in $\epsilon^{-1}$ as described in Ref. 44: $\epsilon^{-1}(k)-1 \to (1-\epsilon(k))/\epsilon'(k)$, where $\epsilon'$ and $\epsilon$ are the dielectric function with and without exchange, and $\epsilon'(k)-1=(\epsilon(k)-1)f(k)$, where $f(k)$ is the Hubbard-Sham exchange factor (Refs. 30 and 45) given explicitly in Ref. 30.

[44] V. Heine and D. Weaire, Phys. Rev. **152**, 603 (1966), Appendix.

[45] J. Hubbard, Proc. Roy. Soc. (London) **A243**, 336 (1958).

[46] A. O. E. Animalu, F. Bonsignori, and V. Bortolani, Nuovo Cimento **44B**, 159 (1966).

[47] W. C. Dunlap and R. L. Watters, Phys. Rev. **92**, 1396 (1953). They find $\epsilon_0=11.8\pm0.2$ for Si.

[48] S. Göttlicher and E. Wölfel, Z. Electrochem. **63**, 859 (1959).

[49] H. Brooks, Trans. AIME **227**, 546 (1963).

[50] M. Born, Proc. Cambridge Phil. Soc. **36**, 160 (1940), and later papers in this series.

[51] M. Born, Ann. Physik 44, 605 (1914).

[52] It is possible to find a diagonal $\epsilon(k)$ which leads to a stable lattice. Such a modified $\epsilon$, which is larger than $\epsilon_F$ with a maximum deviation of 10% near $k=K_F$, has been found in the course of this work. The primary effect is to introduce forces of longer range than in the FE approximation.

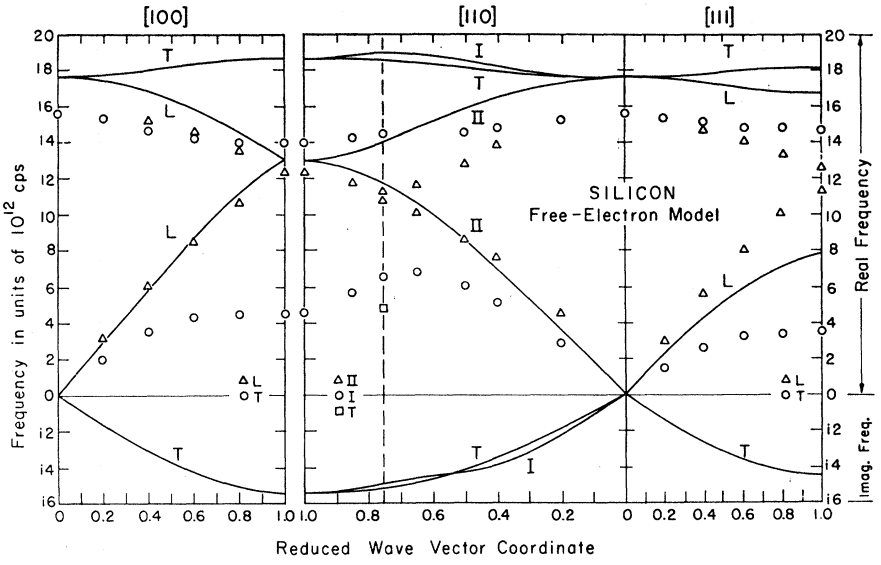


FIG. 1. Phonon dispersion curves for Si calculated from the free-electron model. The ion-core potential used is the MHA model potential described in Sec. V. The points are the neutron scattering data of Dolling (Ref. 15) except for the single [110] TA point measured by Palevsky *et al.* (Ref. 16). The vertical dashed line at 0.75 in the [110] direction indicates the zone boundary. Note that the calculated frequencies of the transverse acoustic modes are imaginary.

The calculation in the FE approximation shows that a statisfactory model for the interatomic forces in Si must take into account at least some effects of the covalent bonding. These effects must be identified in the microscopic formulas and retained in the model. In particular, Born's work[50,51] suggests strongly that noncentral forces must be included. Nevertheless, we note in Fig. 1 that some features of the dispersion curves of Si are given quite well by the FE model. For example, the calculated Raman frequency is only 13% larger than the experimental value. Therefore, in the application of the microscopic theory to Si, we expect to retain many simplifications similar to those of the FE approximation.

## IV. BOND-CHARGE MODEL

Two principal assumptions were employed in the FE approximation: (1) metallic behavior of the dielectric function, $\epsilon_0 \sim 1/q^2$, and (2) neglect of all off-diagonal elements of $\epsilon^{-1}$. Both of these assumptions are incorrect in insulators. All noncentral forces are omitted because of (2), and it was found that this led to the instability against shear in Si. We also require that assumption (1) be omitted so that the method developed here is applicable to crystals with ionic character. (For example, it is desirable to be able to treat Ge and GaAs, the dispersion curves of which are very similar,[18,53] within the same framework.) The acoustic sum rule discussed in Sec. II shows that the relaxations of assumptions (1) and (2) are not independent, because in the long-wavelength limit, some off-diagonal elements of $\epsilon^{-1}$ are related to the magnitude of the macroscopic dielectric constant $\epsilon_0$. Both assumptions are dropped in the present section to derive a more satisfactory model for an insulator.

### A. Phillips's Bond-Charge Model

Let us return to the form of the dynamical matrix in the microscopic theory, Eqs. (2.8) and (2.9). The effective charge $Z^*$ which appears in $\bar{C}_{ss'}{}^{\alpha\beta}(\mathbf{q},2)$, (the subscript $s$ may be omitted in a non-ionic crystal), can be rewritten to exhibit a physical interpretation of the off-diagonal elements of $\epsilon^{-1}$,

$$Z^* = Z + Z^{\mathrm{od}}, \tag{4.1}$$

where $Z$ is the bare-ion–core charge and $Z^{\mathrm{od}}$ is the part of the effective charge which arises entirely from the off-diagonal elements of $\epsilon^{-1}$. The part of the dynamical matrix $\bar{C}_{ss'}{}^{\alpha\beta}(\mathbf{q},2)$ vanishes, of course, for a non-ionic crystal because of the neutrality condition (2.11). However, (2.11) tells us nothing about the spatial distribution of the charge response denoted by $Z^{\mathrm{od}}$, because it refers only to a $q \to 0$ limit. The *total* contribution of the effective charges at arbitrary wave vector need not vanish because the form factors and structure factors for the "off-diagonal" effective charges may differ from those of the bare ion.

The physical arguments for the nature of the off-diagonal charge response in covalent materials are based on Phillips' model of the covalent bond.[10] Phillips suggested that the charge density in a covalent material should be divided into a part linearly screening the ions (much as the linear screening[54] in NFE metals except that the screening is incomplete in an insulator) plus a part concentrated at the bond centers. The additional charge pileup is the result of coherent interference of the Bragg-reflected electron plane-wave states. Phillips argued that the interference is primarily between electron states scattered off neighboring ions. Under this assumption, the maximum in the additional bond-

[53] G. Dolling and J. L. T. Waugh, in *Lattice Dynamics*, edited by R. F. Wallis (Pergamon Press, Ltd., Oxford, 1965), p. 19.

[54] M. H. Cohen and J. C. Phillips, Phys. Rev. **124**, 1818 (1961).

charge density is at the midpoint between neighboring ions in an elemental crystal even when the ions are displaced. Thus, Phillips's model leads to the interpretation that part of the electronic screening of the ion displacements is described by bond charges which are attached to pairs of ions and respond so as to remain midway between them.

The ansatz made in the present paper is that all contributions to the dynamical matrix of the off-diagonal elements of $\epsilon^{-1}$ are replaced by bond-charge interactions with the ions and with other bond charges. This is a reasonable interpretation of Phillips's model because the off-diagonal elements arise from the interference of the plane-wave electron states which the model describes. The neutrality condition (2.11) fixes the magnitude of the effective bond charge $Z_B$,

$$Z_B=\tfrac{1}{2}Z^{\mathrm{od}}=-2\,, \tag{4.2}$$

since there are two bonds per atom. The effective charges defined in (2.10), (4.1), and (4.2) are bare charges. The *total* effective charge, including the screening, is derived by omitting the factor

$$\lim_{q\to 0}\frac{1}{\epsilon^{-1}(\mathbf{q},\mathbf{q})}=\epsilon_0$$

in the definition (2.10). Thus $Z/\epsilon_0$ and $Z^{\mathrm{od}}/\epsilon_0$ are the total effective charges associated with the diagonal and off-diagonal elements of $\epsilon^{-1}$, respectively, and (4.2) is consistent with the bond charge magnitude $-2/\epsilon_0$ predicted by Phillips.

Equation (4.2) is the only requirement that can be derived solely from consideration of the dynamical matrix; however, it is sufficient to demonstrate that the bond charges of Phillips's model are a possible realization of the off-diagonal effective charges found in the general theory. All other assumptions concerning the spatial distribution of the bond-charge response must be introduced as approximations suggested by Phillips's model. It is in these approximations that the specifically covalent character of the off-diagonal screening by the electrons is introduced into the dynamical matrix. In particular, noncentral forces are introduced because the bond charges are not centered on the ion sites. Indeed, in the present account all noncentral forces arise from the bond charges, so that the shear stiffness of the crystal is directly related to $Z_B$ and $\epsilon_0$. A quantitative discussion is given in Secs. VII and VIII, where it is shown that the experimental frequency data provide additional evidence for the bond-charge magnitude predicted by Phillips [Eq. (4.2)].

The model of Phillips for the charge density is in generally good agreement with the results of direct numerical calculations.[55] For a quantitative discussion, based on the actual calculations, of the most important features of the electronic wave functions and how they give rise to the bond charge, see the recent paper by Heine and Jones.[14] The existence of a portion of the valence charge density not spherically symmetric about the ion cores is also established by x-ray scattering measurements on diamond,[48,56] Si,[48,57] and Ge.[58] The x-ray data are most precise in diamond; it verifies approximately Phillips's model in which there is a well-localized bond charge with total charge $-2/\epsilon_0$. The experimental determination of the form factors in Si and Ge is less conclusive (see the discussion by Weiss[59]). Therefore, lacking detailed knowledge of the form factor, the bond charge is here assumed to be a point charge.

Bond-charge models have been used previously for the vibrational properties of covalent materials. The point-bond-charge model for diamond was first proposed and used by Warren[60] (see comment in Sec. IV B). Parr and Borkman[61] utilized bond charges in calculations for diatomic molecules. Also, Simon[62] used a similar model to calculate elastic properties of Ge. In all the above-mentioned work, the bond-charge magnitude was used as an adjustable parameter to fit measured frequencies.

### B. Coulomb Dynamical Matrix

The contribution of the effective charges to the lattice energy, i.e., the force constants, can now be determined. If ion $(s,l)$ is displaced a distance $d\mathbf{R}_{s,l}$, the four bond charges about $(s,l)$ are all displaced by $\frac{1}{2}d\mathbf{R}_{s,l}$ and similarly for ion $(s',l')$. To obtain the force constant $C_{ss'}{}^{\alpha\beta}(l-l')$, we must simply add the interactions of the five charges at $(s,l)$ (the ion and four bond charges) with the five charges at ion $(s',l')$. The interactions among the charges are classified as ion-ion, ion-bond, and bond-bond.

The force constant $C_{ss'}{}^{\alpha\beta}(l-l')$ is here divided into the Coulombic and non-Coulombic parts:

$$C_{ss'}{}^{\alpha\beta}(l-l')={}^{\mathrm{C}}C_{ss'}{}^{\alpha\beta}(l-l')+{}^{\mathrm{nC}}C_{ss'}{}^{\alpha\beta}(l-l')\,. \tag{4.3}$$

The Coulombic part is derived from the Coulomb interactions among the charges[63]

$$Z_1Z_2e^2/\epsilon_0 r\,, \tag{4.4}$$

[55] I. Goroff and L. Kleinman, Phys. Rev. **164**, 1100 (1967); L. Kleinman and J. C. Phillips, *ibid.* **125**, 819 (1962).

[56] R. Brill, Acta Cryst. **13**, 275 (1960).

[57] H. Hattori, H. Kuriyama, and T. Katayawa, J. Phys. Soc. Japan **20**, 988 (1965).

[58] J. J. Demarco and R. J. Weiss, Phys. Rev. **137**, A1869 (1965); L. D. Jennings, Bull. Am. Phys. Soc. **13**, 491 (1968).

[59] R. J. Weiss, Acta Cryst. (to be published).

[60] J. L. Warren, Brookhaven National Laboratory Report No. BNL-940(C-45), 1965, p. 88 (unpublished).

[61] R. G. Parr and R. F. Borkman, J. Chem. Phys. **49**, 1055 (1968); R. F. Borkman, G. Simons, and R. G. Parr, *ibid.* **50**, 58 (1968).

[62] G. Simon, J. Phys. Chem. Solids **28**, 2349 (1967).

[63] Naively, using the total bond-charge magnitude $-2/\epsilon_0$, one might expect the bond-bond interaction, for example, to be proportional to $(-2/\epsilon_0)^2$. However, this would not take into account the medium screening of the bond charges which contributes an addition factor of $\epsilon_0$ to arrive at the result (4.5).

where $Z_1$ and $Z_2$ take the value $Z$ or $Z_B$ for the ion core or bond charge, respectively, and $r$ is the relevant separation. The non-Coulombic part arises from the short-range ion-ion forces which are determined by the dispersion of the diagonal part of the inverse dielectric function $\epsilon^{-1}(\mathbf{q}+\mathbf{K}, \mathbf{q}+\mathbf{K})-1/\epsilon_0$, and are described in Sec. V. No short-range corrections are included in the ion-bond and bond-bond interactions. This is a reasonable first approximation because the total bond charge contains only a small fraction of the electrons, and hence it need not be treated as accurately as the ion-ion terms.

The Coulombic force constant now may be written as

$$^{C}C_{ss'}{}^{\alpha\beta}(l)=-\frac{e^2}{\epsilon_0}\sum_{i,j=1}^{5}W_iW_jZ_iZ_j \times f_{\alpha\beta}(\mathbf{R}_{sl}-\mathbf{R}_{s'0}+\mathbf{R}_i(s)-\mathbf{R}_j(s')), \quad (4.5)$$

where

$$f_{\alpha\beta}(r)=\frac{\partial^2}{\partial r^\alpha \partial r^\beta}\frac{1}{|r|}, \quad (4.6)$$

$$\begin{aligned} &W_i=\tfrac{1}{2}, \quad Z_i=Z_B, \quad i\leqslant 4 \\ &W_i=1, \quad Z_i=Z, \quad i=5 \end{aligned} \quad (4.7)$$

$\mathbf{R}_i(s)$ = bond positions about ion $s$ for $i=1, 2, 3, 4$, and $R_5(s)=0$. The vectors $\mathbf{R}_i(s)$ for $i\leqslant 4$ are shown in Fig. 2 and are listed for convenience:

$$\begin{aligned} &\mathbf{R}_1(1)=-\mathbf{R}_1(2)=\tfrac{1}{8}a(1,1,1), \\ &\mathbf{R}_2(1)=-\mathbf{R}_2(2)=\tfrac{1}{8}a(1,-1,-1), \\ &\mathbf{R}_3(1)=-\mathbf{R}_3(2)=\tfrac{1}{8}a(-1,1,-1), \\ &\mathbf{R}_4(1)=-\mathbf{R}_4(2)=\tfrac{1}{8}a(-1,-1,1), \end{aligned} \quad (4.8)$$

where $a$ is the conventional cube edge which is 5.430 Å in Si. The asymptotic form of the Coulomb force constants (4.5) are a particular model of the quadrupole-quadrupole forces first suggested by Lax.[64]

Equation (4.5) must be modified in the case where $(s,l)$ denotes a nearest neighbor of $(s,0)$ with the common bond labeled $i_0$. The correct force constant is (4.5) with the term $i=j=i_0$ replaced by the second derivative of the total energy with respect to the position of bond charge $i_0$, which may be shown to be

$$\frac{e^2}{\epsilon_0}\tfrac{1}{4}Z_B\Big[Z\sum_{s''l''}f_{\alpha\beta}(\mathbf{R}_{s'0}-\mathbf{R}_{s''l''}+\mathbf{R}_{i_0}(s')) +Z_B\sum_{k,l''}{}'f_{\alpha\beta}(\mathbf{R}_{s'0}-\mathbf{R}_{s'l''}+\mathbf{R}_{i_0}(s')-R_k(s'))\Big], \quad (4.9)$$

the factor of $\frac{1}{4}$ coming from the $W_iW_j$ coefficient in (4.5). Similarly, the self-force constant $^{C}C_{ss}{}^{\alpha\beta}(0)$ is modified, but it is not needed in the dynamical matrix.

The dynamical matrix for the Coulomb forces is derived from (4.5) and (4.9); after a small amount of manipulation it becomes

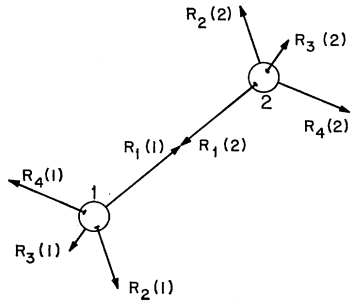


FIG. 2. Bond-charge positions in the diamond lattice. The atoms 1 and 2 in the unit cell are shown along with the four bond-charge positions $\mathbf{R}_i(s)$ about each atom.

$$^{C}\bar{C}_{ss'}{}^{\alpha\beta}(\mathbf{q})=\frac{e^2}{\epsilon_0}\sum_{i,j=1}^{5}W_iW_jZ_iZ_j \times\{e^{i\mathbf{q}\cdot[\mathbf{R}_i(s)-\mathbf{R}_j(s')]}G_{\alpha\beta}(\mathbf{q}, \mathbf{R}_s+\mathbf{R}_i(s)-\mathbf{R}_{s'}-\mathbf{R}_j(s')) -(1-\delta_{ss'})(1-\delta_{i,5})e^{-2i\mathbf{q}\cdot\mathbf{R}_i(s)}G_{\alpha\beta}(0, \mathbf{R}_i(s)-\mathbf{R}_j(s))\}, \quad (4.10)$$

where

$$G_{\alpha\beta}(\mathbf{q},\mathbf{r})=-\sum_l{}'f_{\alpha\beta}(\mathbf{r}-\mathbf{R}_l)e^{-i\mathbf{q}\cdot(\mathbf{r}-\mathbf{R}_l)}, \quad (4.11)$$

which is evaluated by the Ewald transformation.[1,37] The second term in the brackets in (4.10) was omitted by Warren.[60] This term involves $G_{\alpha\beta}(\mathbf{q}=0)$, but it has a $\mathbf{q}$-dependent coefficient, because the bond charges are not located at the ion sites, and must therefore be included in $^{C}\bar{C}$.

## V. NON-COULOMBIC DYNAMICAL MATRIX

The non-Coulombic dynamical matrix is given by

$$^{nC}\bar{C}_{ss'}{}^{\alpha\beta}(\mathbf{q})=\frac{\Omega}{4\pi e^2}\sum_{\mathbf{K}}(\mathbf{q}+\mathbf{K})^\alpha(\mathbf{q}+\mathbf{K})^\beta \times|\mathbf{q}+\mathbf{K}|^2[v(|\mathbf{q}+\mathbf{K}|)]^2 \times[\epsilon^{-1}(\mathbf{q}+\mathbf{K}, \mathbf{q}+\mathbf{K})-1]e^{i\mathbf{K}\cdot(\mathbf{R}_s-\mathbf{R}_{s'})} +(4\pi e^2/\Omega)Z^2(1-1/\epsilon_0)G_{\alpha\beta}(\mathbf{q}, \mathbf{R}_s-\mathbf{R}_{s'}), \quad (5.1)$$

where (2.5), (4.3), and (4.4) have been used. In the second term on the right-hand side of (5.1), the factor $1/\epsilon_0$ subtracts from $^{nC}C$ the long-range part of the ion-ion interaction which has already been included in $^{C}C$, as defined in the previous section. We are left with the problem of calculating $^{nC}C$, which involves only the ion-core potential $v(|\mathbf{q}+\mathbf{K}|)$ (the subscript $s$ may be dropped for elemental crystals), and the diagonal part $\epsilon^{-1}(\mathbf{q}+\mathbf{K}, \mathbf{q}+\mathbf{K})$. We must specify only these two functions—a much simpler problem than the one with which we started, which involved the entire matrix of the inverse dielectric function.

[64] M. Lax, Phys. Rev. Letters **1**, 133 (1958).

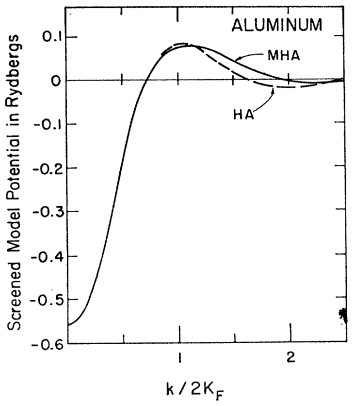


FIG. 3. Screened model potential in aluminum. The solid curve is the modified Heine-Abarenkov (MHA) model potential derived from Table I of Animalu *et al.* (Ref. 46). The dashed curve is the Heine-Abarenkov (HA) potential tabulated in Ref. 32.

The pseudopotential form factor is arrived at by comparison with the pseudopotential calculated for Al by Animalu *et al.*,[46] via a modified Heine-Abarenkov (here called MHA) method. The Al ion-core form factor is of interest because the $Si^{+4}$ and $Al^{+3}$ ion cores are identical except for the difference in the nuclear charge; any approximation which applies to the ion core of Al should also apply to the $Si^{+4}$ core. The potential $v_{MHA}$ for Al can be calculated from Table I of Animalu *et al.*,[46] and is shown in Fig. 3 along with the Heine-Abarenkov potential[32,65] $v_{HA}$. The primary point is that $v_{MHA}$ and $v_{HA}$ differ only at large wave number ($k>2K_F$), where $v_{MHA}$ is more strongly damped. (Here $k$ denotes a variable that extends over all reciprocal space.) The MHA pseudopotential for Al was shown[46] to yield phonon dispersion curves in good agreement with experiment ($\sim 10\%$ maximum error). The final potential form factor for $Si^{+4}$ (also termed MHA), derived from the HA form factor for Si by a comparison with the Al case, is shown in Fig. 4. Note that here we have plotted the bare ion-core potential multiplied by $k^2/4\pi Ze^2$. The bare HA potential is determined by multiplying the tabulated screened HA potential[32,65] by the Hubbard-Sham dielectric function.[30,65] It was found in the course of the present work that only very small changes in the dispersion curves result from making the potential go smoothly to zero near the second node as is done in the final potential. A similar form factor has been used for calculating phonon dispersion curves in metallic Sn.[66]

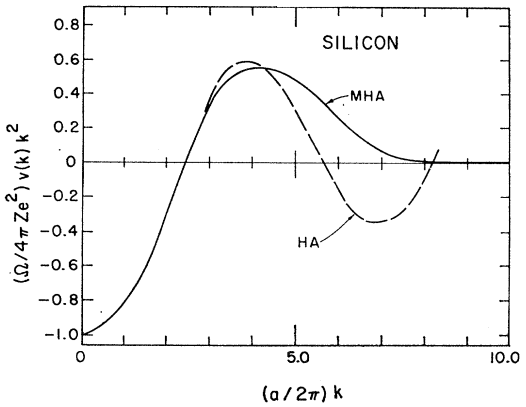


FIG. 4. $(\Omega/4\pi Ze^2)v(k)k^2$, where $v$ is the bare-ion–core potential for Si. The solid curve is the modified Heine-Abarenkov (MHA) potential used in the calculation of phonon dispersion curves shown in Fig. 6. The dashed curve is for the Heine-Abarenkov (HA) potential derived from the tables of Ref. 32.

[65] V. Heine and I. Abarenkov, Phil. Mag. **9**, 451 (1964).

It is convenient to define an "effective" dielectric function $\epsilon_{\text{eff}}(\mathbf{q}+\mathbf{K})$ by

$$\epsilon^{-1}(\mathbf{q}+\mathbf{K},\,\mathbf{q}+\mathbf{K})=1/\epsilon_{\text{eff}}(\mathbf{q}+\mathbf{K}). \tag{5.2}$$

Equation (5.2) shows that, strictly speaking, $\epsilon_{\text{eff}}$ can be determined only by calculating the entire $\epsilon$ matrix. However, we have chosen to use the $\epsilon_{\text{eff}}$ calculated by Srinivasan[67] from Penn's idealized isotropic model[68] of the electronic wave functions in a semiconductor. The functional form of $\epsilon_{\text{Penn}}(|\mathbf{q}+\mathbf{K}|)$ is derived from the expressions for the diagonal part of the dielectric function $\epsilon(\mathbf{q}+\mathbf{K},\,\mathbf{q}+\mathbf{K})$, but the parameters are chosen so that it is really appropriate for the effective dielectric function, as defined in (5.2) [that is, $\epsilon_{\text{Penn}}(0)=\epsilon_0$], rather than for the dielectric function itself.

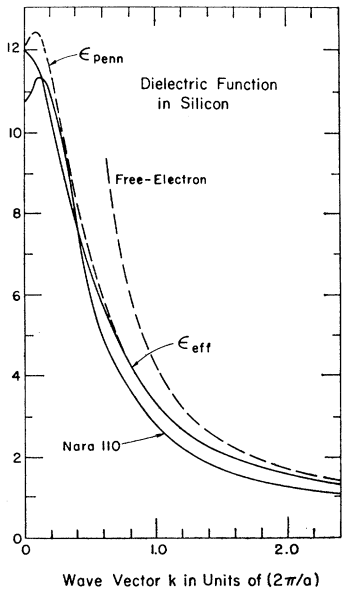


FIG. 5. Dielectric function in silicon as a function of wave number $k$: (1) the free-electron function, (2) $\epsilon_{\text{Penn}}$ as calculated by Srinivasan (Ref. 67), (3) $\epsilon_{\text{Nara}}$ for the [110] direction (Ref. 69), and (4) $\epsilon_{\text{eff}}$, which is equal to $\epsilon_{\text{Penn}}$ over the range shown except that it is adjusted at small $k$ to fit the elastic constant $C_{11}$.

[66] E. G. Brovman and Yu Kagan, Zh. Eksperim. i Teor. Fiz. **52**, 557 (1967) [English transl.: Soviet Phys.—JETP **25**, 365 (1967)].
[67] G. Srinivasan, Phys. Rev. **178**, 1244 (1969).
[68] D. R. Penn, Phys. Rev. **128**, 2093 (1962).

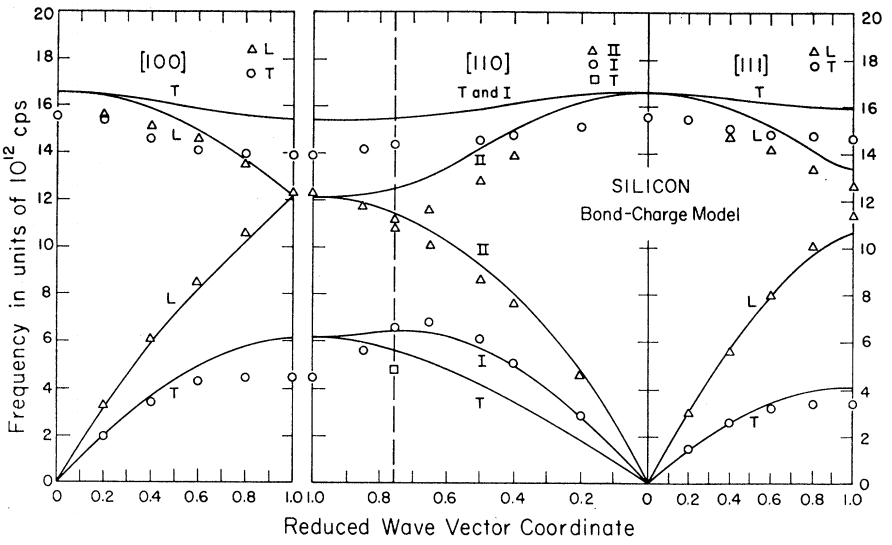


FIG. 6. Phonon dispersion curves for Si calculated from the bond-charge model. The ion-core potential used is the MHA model potential in Fig. 4 and the effective dielectric function is $\epsilon_{\rm eff}(k)$ given in Fig. 5. The points are the results of the neutron scattering measurements of Dolling (Ref. 15) except for the single [110] TA point from Palevsky *et al.* (Ref. 16). The vertical dashed line of 0.75 in the [110] direction indicates the zone boundary.

The isotropic function $\epsilon_{\rm Penn}(k)$ for Si is given in Fig. 5 along with the dielectric function $\epsilon(\mathbf{q}+\mathbf{K}, \mathbf{q}+\mathbf{K})$ calculated by Nara[69] from a realistic band structure. Nara found $\epsilon(\mathbf{q}+\mathbf{K}, \mathbf{q}+\mathbf{K})$ to be remarkably isotropic; his result for the [110] direction is shown. The agreement between the two functions lends support to the validity of Penn's model. It is in the assumption of the Penn form for $\epsilon_{\rm eff}(k)$ that we have used the NFE character of Si. Such an approximation for $\epsilon_{\rm eff}(k)$ would be less appropriate for substances with larger band gaps, e.g., diamond. The simple form for $\epsilon_{\rm eff}$ plays the same role in making the present model tractable as does the FE dielectric function in the calculations for NFE metals.

We have included the exchange corrections just as was described in Ref. 43 for the FE case. The correct dielectric constant $\epsilon_0$ is still obtained because the exchange correction vanishes as $k \to 0$, and the resulting ion-electron-ion interaction should be valid for large $k$ because the assumptions for the form of $\epsilon_{\rm eff}$ with exchange are valid as $\epsilon_{\rm eff} \to \epsilon_{\rm free}$. But for $k$ near zero, the results are invalid; Penn's model is poor, and the many-body correction employed is qualitatively wrong because it vanishes for $k \to 0$. Therefore, the effective dielectric function has been regarded as an adjustable function at small $k$ (within the first Brillouin zone (BZ) only). This is the only adjustment in the present calculation. It affects only longitudinal acoustic modes and here it is used to fit the measured elastic constant $C_{11}$. The resulting function is labeled $\epsilon_{\rm eff}$ in Fig. 5. It turns out that in the adjusted function there is no "hump" at small $k$ as found by both Nara[69] and Penn.[68] Such a hump would make $C_{11}$ negative and cannot be reconciled with the bond-charge model.

The function $\epsilon_{\rm eff}(k)$ as used in this paper is defined for large $k$ by smoothly extending the curve shown to the FE function $\epsilon_F(k)$. Calculations have also been carried out for the slightly different function calculated by Srinivasan[67] for large $k$ with only minor changes in the results. Both the effective dielectric function and the ion-core potential (multiplied by $k^2$) were tabulated. The needed sums in the dynamical matrix (5.1) were calculated by a quadratic interpolation procedure.

[69] H. Nara, J. Phys. Soc. Japan **20**, 778 (1965).

## VI. RESULTS

The calculation of the phonon frequencies using the dynamical matrix given in (4.10) and (5.1) has been carried out for phonon wave vector $q$ along the symmetry directions [100], [110], and [111]. The ion-core potential used is $v_{\rm MHA}$ given in Fig. 4, and the effective dielectric function is $\epsilon_{\rm eff}(k)$ of Fig. 5. The resulting phonon dispersion curves are displayed as solid lines in Fig. 6, and the calculated elastic constants are given in the third row of Table I. The only adjustment used to fit the experimental phonon frequencies is the curvature of $\epsilon_{\rm eff}(k)$ at $k=0$, which determines the dielectric function $\epsilon_{\rm eff}(k)$ inside the first BZ. The adjustment affects only LA modes inside the BZ; no fitting is involved in

TABLE I. Elastic constants in Si. The first row gives the experimental constants, the second row the results of the free-electron model described in Sec. III, and the remaining rows the results of various bond-charge-model calculations. The values in parentheses indicate the results if $C_{11}$ is fitted.

| | $C_{11}$ | $C_{44}$ | $C_{12}$ | $C_{11}-C_{12}$ | $B$ |
|---|---|---|---|---|---|
| Experiment[a] | 1.66 | 0.80 | 0.64 | 1.02 | 0.98 |
| FE | 1.49 | −0.42 | 2.07 | −0.58 | 1.89 |
| $v_{\rm MHA}$, $\epsilon_{\rm eff}$ | 1.66 | 0.75 | 0.96 | 0.70 | 1.19 |
| $v_{\rm HA}$, $\epsilon_{\rm eff}$ | 1.20 | 0.34 | 0.92 | 0.28 | 1.01 |
| | (1.66) | | (1.38) | | (1.47) |
| $v_{\rm MHA}$, $\epsilon_{\rm eff}$[b] | 2.84 | 0.57 | 2.44 | 0.40 | 2.57 |
| | (1.66) | | (1.26) | | (1.39) |

[a] H. B. Huntington, in *Solid State Physics*, edited by F. Seitz and D. Turnbull (Academic Press Inc., New York, 1958), Vol. 7, p. 213.
[b] Omitting Hubbard-Sham exchange factor.

any of the other modes, or in the LA modes at the zone boundary.

Comparison of Figs. 1 and 6 shows the modifications in the calculated phonon dispersion curves resulting from replacing the FE screening by the bond-charge-model screening for the same ion-core potential $v_{\mathrm{MHA}}$. In the bond-charge model, all TA modes have real frequencies, showing that the stability of the crystal against shear has been achieved. In addition, all optic mode shapes are now much closer to the experimental shapes in the FE approach, e.g., the TO-mode frequencies decrease as $|\mathbf{q}|$ increases in contrast with the behavior of these modes in the FE model.

The results now are generally in good agreement with experiment. With the exception of the TA modes, the worst error is 11% in the TO mode at $X$, the [100] zone boundary. The calculated Raman frequency is 16.6 $\times 10^{12}$ cps, which is 6% higher than the experimental value 15.66.[70] All modes have qualitatively correct shapes except the [110] II optic mode, which does not show the minimum near the zone boundary found experimentally. One feature, the crossing of the LO and TO curves along the [100] direction, is not found in any of the present calculations and remains unexplained in the bond-charge model.

The worst deviation from the experimental frequencies is for the TA mode at $X$, where the calculated frequency is 36% too large. The [100] TA mode agrees with experiment very well in the elastic region, but does not show the characteristic flattening found experimentally. This discrepancy is caused to a large extent by the point-charge assumption. The results of Sec. VIII show that the TA-mode shape would be improved by the introduction of a bond-charge form factor $Z_B(k)$.

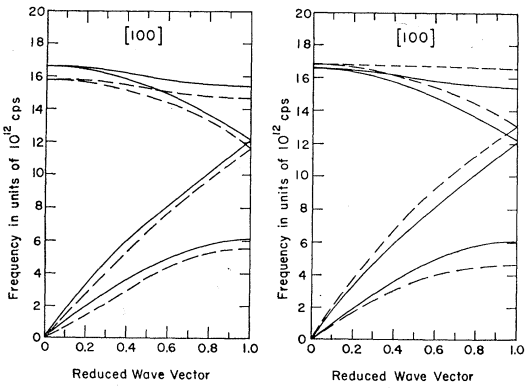


FIG. 7. Comparison of dispersion curves along the [100] direction. (a) The solid curves are calculated from $v_{\mathrm{MHA}}$ and $\epsilon_{\mathrm{eff}}$ (same as Fig. 6); the dashed curves are calculated from $v_{\mathrm{HA}}$ and the same $\epsilon_{\mathrm{eff}}$. (b) The solid curves are calculated from $v_{\mathrm{MHA}}$ and $\epsilon_{\mathrm{eff}}$ just as in part (a); the dashed curves are calculated from the same potential and dielectric function, but omitting the Hubbard-Sham exchange factor.

[70] F. A. Johnson and R. Loudon, Proc. Roy. Soc. (London) **A281**, 274 (1968).

In general, the fractional deviation of the calculated frequencies from the experimental values is comparable to the results[46] for Al—roughly 10% errors. Because the frequencies of the transverse modes in Si are so low, indicating a large amount of cancellation among the forces involved, the errors of ~30% in the transverse modes are not surprising. We can conclude that, although there is much more remaining to be understood in the dispersion curves of Si, the calculation of phonon frequencies for Si based on the bond-charge model of screening is roughly as accurate as the calculation[46] for Al based on FE screening.

The sensitivity of the results has been tested by employing several variations in the potential and effective dielectric function. Comparison of the results using $v_{\mathrm{MHA}}$ and $v_{\mathrm{HA}}$ with the same $\epsilon_{\mathrm{eff}}(k)$ are shown in Table I and in Fig. 7(a) for the [100] direction. (Note that if $C_{11}$ is to be fitted, $\epsilon_{\mathrm{eff}}$ must be modified slightly,

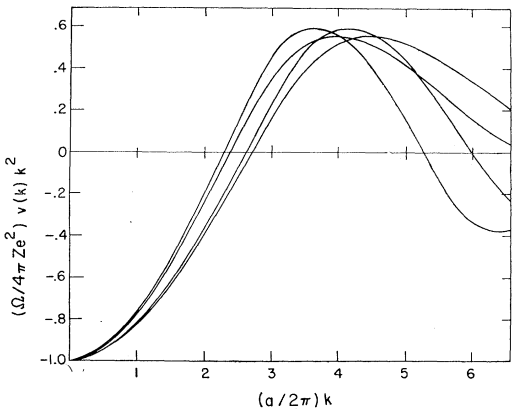


FIG. 8. Family of ion-core potential form factors for Si. The range of the form factor indicated by this family of curves has been shown to yield qualitatively the same dispersion curves (see discussion in text).

which would yield the elastic constants shown in parentheses in the fourth row of Table I.) We have also employed the potentials shown in Fig. 4 scaled along the $k$ axis, the primary effect of which is to shift the optic modes rigidly. The range of the potentials which leave the Raman frequency within 15% of the experimental value is shown in Fig. 8. The important conclusion is that the family of potentials shown in Fig. 8, along with other intermediate functions, all lead to qualitatively the same phonon dispersion curves. Also for this family of curves, all the conclusions about the inadequacy of the FE approximation remain intact.

As an example of the variation of the frequencies if $\epsilon_{\mathrm{eff}}(k)$ is changed, a calculation was carried out with the exchange factor set equal to 1, i.e., no exchange correction, which is equivalent to lowering the $\epsilon_{\mathrm{eff}}(k)$ curve with a maximum deviation of 10% at $k=K_F$. The changes in elastic constants and frequencies are shown in Table I and Fig. 7(b), in which case $v_{\mathrm{MHA}}$ was used.

Again the fitted elastic constants are given in parentheses.

The various calculations show that the primary features of the dispersion curves do not depend on the detailed form of the functions employed. Better agreement with experiment could be achieved by adjusting $v$ and $\epsilon_{\text{eff}}$ (as well as parametrizing the form factor of the bond charge and the manner in which it moves as the ions are displaced), but no such systematic fitting of the phonon frequencies has been attempted here.

## VII. CALCULATED FORCE CONSTANTS IN REAL SPACE

We now turn to the form of the forces in real space, i.e., the force constants $C_{ss'}{}^{\alpha\beta}(l-l')$ in the bond-charge model. The transformation to real space, which is a cumbersome and unnecessary step in the actual calculation of the dispersion curves, affords a much clearer picture of the operative forces in the crystal. The Coulombic forces have already been described in real space and given in (4.5) and (4.9). All that must be done

TABLE II. Calculated functions $F_1(r)$ and $F_2(r)$ evaluated at the first four-neighbor separations. The non-Coulombic force constants are determined from this table and Eq. (7.2).

| | Neighbor | $v_{\text{MHA}}$ $\epsilon_{\text{eff}}$ | $v_{\text{HA}}$ $\epsilon_{\text{eff}}$ |
|---|---|---|---|
| $F_1$ | 1 | −0.064 | −0.059 |
| | 2 | −0.004 | −0.002 |
| | 3 | 0.001 | 0.001 |
| | 4 | 0.004 | −0.004 |
| $F_2$ | 1 | 0.788 | 0.743 |
| | 2 | 0.015 | 0.032 |
| | 3 | 0.017 | −0.027 |
| | 4 | −0.025 | 0.022 |

is to transform the non-Coulombic dynamical matrix (5.1) into the real-space force constants.

Because the non-Coulombic forces are purely central, they may be derived from some scalar potential $\varphi(r)$ and may be written

$$ {}^{\text{nC}}C_{ss'}{}^{\alpha\beta}(l-l') = -\frac{Z^2e^2}{r_l}\left([F_2(r)-F_1(r)]\frac{r^\alpha r^\beta}{r^2}+\delta_{\alpha\beta}F_1(r)\right). \tag{7.1}$$

From (5.1) and using Ref. 43, it may readily be shown that for $(s,l)\neq(s',l')$, the quantities $F_1(r)$ and $F_2(r)$ are given by

$$F_1(r)=r^2\varphi'(r)/Z^2e^2=(1/\epsilon_0-1) +\frac{2r}{\pi}\int_0^\infty dk\, W(k)\left(\frac{\sin kr}{kr}-\cos kr\right) \tag{7.2a}$$

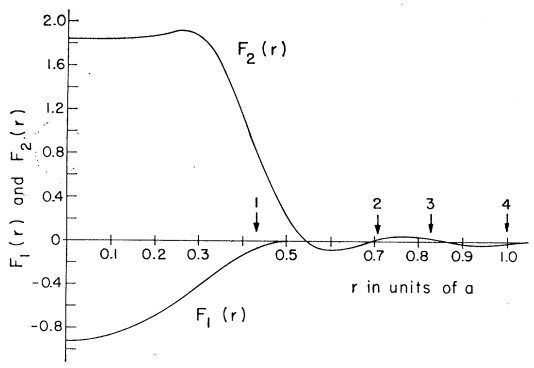


FIG. 9. Functions $F_1(r)$ and $F_2(r)$ which determine the force constants for the non-Coulombic forces. These curves are calculated from $v_{\text{MHA}}$ and $\epsilon_{\text{eff}}$ with the Hubbard-Sham exchange correction. The arrows indicate the near-neighbor separations.

and

$$F_2(r)=r^3\varphi''(r)/Z^2e^2=-2F_1(r) +\frac{2r}{\pi}\int_0^\infty dk\, W(k)kr\sin kr, \tag{7.2b}$$

where

$$W(k)=\left(\frac{k^2v(k)}{4\pi Ze^2}\right)^2\left(\frac{\epsilon_{\text{eff}}(k)-1}{[\epsilon_{\text{eff}}(k)-1]f(k)+1}\right). \tag{7.3}$$

The integrals in (7.2) have been evaluated numerically using $\epsilon_{\text{eff}}$, with $v_{\text{MHA}}$ and $v_{\text{HA}}$. The values of $F_1(r)$ and $F_2(r)$ at the near-neighbor positions are listed in Table II, and the entire curves for the case involving $v_{\text{MHA}}$ are shown in Fig. 9. The forms of $F_1$ and $F_2$ are very similar in the two cases, but the nodes are displaced and the amplitudes changed somewhat, leading to large differences in the values for neighbors beyond the first.

The primary result is that both $F_1(r)$ and $F_2(r)$ are small at and beyond the second neighbor separation. It is evident that the bond-charge-model calculation presented above is equivalent to adding central non-Coulombic forces that extend for only a few neighbors to the Coulombic forces. [The force constant is further diminished by the factor $r^{-3}$ in (7.1).] Also, it is seen that the present knowledge of the pseudopotential and the effective dielectric function is not sufficient to predict accurately the non-Coulombic force constants for the second and more distant neighbors. Therefore, all results which depend sensitively on these force constants cannot be expected to be well described in the present calculations.

The fractional contribution of the various forces to the frequencies squared is exhibited in Table III in the case of the calculation involving $v_{\text{MHA}}$ and $\epsilon_{\text{eff}}$. The forces are divided into (1) Coulombic, (2) first-neighbor non-Coulombic, and (3) the remaining non-Coulombic forces. The contributions are shown for the four frequencies at the symmetry points $\Gamma$ and $X$, and for

TABLE III. Fractional contributions to special frequencies from the various types of forces in the bond-charge model. The non-Coulombic forces are divided into first-neighbor forces and those for all the more distant neighbors.

| Mode or elastic constant | Coulomb | Non-Coulomb First | Non-Coulomb Beyond first |
|---|---|---|---|
| $\omega_0^2(\Gamma)$ | 0 | 0.98 | 0.02 |
| $\omega_{TA}^2(X)$ | 1.96 | −1.14 | 0.18 |
| $\omega_{TO}^2(X)$ | −0.31 | 1.30 | 0.01 |
| $\omega_L^2(X)$ | 0.03 | 0.92 | 0.05 |
| $C_{11}$ | 0.05 | 0.64 | 0.31 |
| $C_{12}$ | −0.94 | 1.71 | 0.24 |
| $C_{11}-C_{12}$ | 1.53 | −0.94 | 0.41 |
| $B$ | −0.50 | 1.23 | 0.27 |
| $C_{44}$ | 10.45 | −9.84 | 0.39 |

several combinations of elastic constants. The Coulombic forces do not contribute to the Raman frequency $\omega_0(\Gamma)$ as may be derived from simple arguments. In general, the Coulombic forces play only a small role in the longitudinal modes, but are essential in the transverse modes. As exemplified by the shear elastic constants $C_{44}$ and $C_{11}$–$C_{12}$ and $\omega_{TA}(X)$, the nearest-neighbor non-Coulombic forces tend to make the lattice unstable, but the Coulombic forces are sufficient to achieve stability. Also, as illustrated by $\omega_{TO}(X)$, it is the Coulombic forces that bring down the TO frequency at the zone boundary. Thus the bond-charge-model noncentral Coulombic forces are clearly responsible for the stability of the lattice, and for the improvement of the dispersion curves, in comparison to the results of the FE approximation.

The only results listed in Table III which depend greatly on the non-Coulombic forces past the first neighbor are the elastic constants and, to a lesser extent, $\omega_{TA}(X)$. Thus, these are the features which are most sensitive to the detailed form of the ion-core form factor and effective dielectric function. It should be emphasized that Table III lists the division of forces in the particular calculation using $v_{MHA}$ and $\epsilon_{eff}$; the distribution in Table III, especially for the elastic constants, will change somewhat for other choices of these functions.

## VIII. SIMPLE BOND-CHARGE (SBC) MODEL

The results of Sec. VII show that the major features of the Si dispersion curves can be described by a model with only the Coulombic forces and a nearest-neighbor non-Coulombic central force. In this section, we examine such a model, which is here called the simple-bond-charge (SBC) model.[71] The advantage of this simplification is that it allows a useful characterization of the forces and is readily extendable to all the diamond-structure crystals. Because there are only purely Coulombic and nearest-neighbor non-Coulombic forces, the SBC model has many aspects in common with the rigid-ion models for highly ionic crystals. The only essential difference is in the spatial locations of the effective charges.

Let us define the energy function per atom, which describes the changes in energy in the SBC model for small deviations of the lattice constant from equilibrium:

$$E(\tau)=2\varphi(\tau)-\tfrac{1}{2}\alpha(2Z_B'e)^2/\epsilon_0\tau. \tag{8.1}$$

Here $\tau$ is the nearest-neighbor separation, $\varphi$ is an arbitrary potential function, and $\alpha$ is the Madelung constant for the system of "bare" charges $-2Z_B'e$ at the ion sites and $Z_B'e$ at the bond sites. In the SBC model, the charge $Z_B'$ is regarded as a parameter which may be compared with the value $Z_B=-2$ used above. The constant $\alpha$ has been evaluated numerically and found to be

$$\alpha=4.453. \tag{8.2}$$

If the crystal is to be in equilibrium at the given lattice constant, we must have

$$\frac{dE}{d\tau}=2\varphi'(\tau)+\frac{\tfrac{1}{2}\alpha(2Z_B'e)^2}{\epsilon_0\tau^2}=0, \tag{8.3}$$

which fixes the first derivative of $\varphi$.

Following the results of the previous section for Si, we now assume that $\varphi(\tau)$ is simply a two-body nearest-neighbor potential. In general, $\varphi(\tau)$ must incorporate such volume effects as the electron gas compressibility; here we are assuming that the local electron density is a function only of the local atomic displacements, so that $\varphi(\tau)$ has this simple interpretation. To allow direct comparison with Sec. VII, let us define

$$F_1^{SBC}=\tau^2\varphi'(\tau)/(Ze)^2 \tag{8.4a}$$

and

$$F_2^{SBC}=\tau^3\varphi''(\tau)/(Ze)^2. \tag{8.4b}$$

The equilibrium condition fixes $F_1^{SBC}$ to be

$$F_1^{SBC}=-(\alpha/\epsilon_0)(Z_B'/Z)^2. \tag{8.5}$$

Therefore, in the SBC model there are only two free parameters, the charge $Z_B'$ and the constant $F_2^{SBC}$ which describes the non-Coulombic forces.

It is instructive to see how the parameters $F_2^{SBC}$ and $Z_B'$ contribute to special frequencies in the BZ. Expressions can be easily derived for representative elastic

TABLE IV. Comparison of the observed bulk modulus with that calculated from the Raman frequency using Eq. (8.7).

| Element | $B_{obs}/B_{calc}$ |
|---|---|
| Diamond | 1.004 |
| Si | 0.942 |
| Ge | 0.894 |

[71] In a previous paper [R. M. Martin, Chem. Phys. Letters **2**, 268 (1968)], the name "simple-bond-charge model" was applied to a model in which the nearest-neighbor non-Coulombic force had a specific form. No such assumption on this force is made here. Several aspects of the present discussion were given in the above-mentioned reference.

constants and frequencies. Let us define the parameters $R=(256/9\sqrt{3})F_2^{SBC}$ and $S=Z_B'^2/\epsilon_0$. Expressing frequencies squared in units of $e^2/\Omega M$ and elastic constants in units of $e^2/\Omega a$, we find

$$\omega_0^2=8(R-9.140S), \tag{8.6a}$$

$$\omega_L^2(X)=4(R-8.100S), \tag{8.6b}$$

$$\omega_{TA}^2(X)=12.580S, \tag{8.6c}$$

$$\omega_{TO}^2(X)=8(R-11.232S), \tag{8.6d}$$

$$B=R-9.140S, \tag{8.6e}$$

$$C_{11}=R-6.964S, \tag{8.6f}$$

$$C_{11}-C_{12}=3.264S. \tag{8.6g}$$

Comparison of Eqs. (8.6a) and (8.6e) shows that in the SBC model there is a relation between the bulk modulus and Raman frequency:

$$8aB=M\omega_0^2. \tag{8.7}$$

Equation (8.7) is a special case of the relation derived by Szigetti[72] for ionic crystals. In Table IV, the relation is tested by the experimental values for diamond, Si, and Ge. The relation is very well satisfied in diamond, but is progressively worse for Si and Ge. The most probable reason for the deviations from (8.7) is that the assumption that $\varphi$ can be regarded as a simple two-body interaction is less valid as the electron density becomes more metallike in Si and Ge. However, the deviations are small (of the same order as the deviations found by Szigetti[72] for ionic crystals), and we may expect the SBC model to describe correctly the gross features of the dispersion curves.

The second conclusion to be drawn from the formulas (8.6) is that both $C_{11}$–$C_{12}$ and $\omega_{TA}(X)$ depend only on $S$ and not on $R$. However, $R$ appears in all the other frequencies, and in fact dominates the optic frequencies. Thus, for example, the relation of $\omega_{TA}(X)$ to the Raman frequency $\omega_0$ is fixed by the ratio of $S$ to $R$.

Let us choose the parameters $Z_B'$ and $F_2^{SBC}$ by fitting the experimental frequencies $\omega_0(\Gamma)$ and $\omega_{TA}(X)$. The results are shown in Table V for diamond, Si ,Ge, and grey Sn. Also given are the dielectric constant $\epsilon_0$ and $S=Z_B'^2/\epsilon_0$.

TABLE V. Parameters $F_2^{SBC}$ and $Z_B'$ in the SBC model. Also given is the macroscopic dielectric constant $\epsilon_0$ and $S=Z_B'^2/\epsilon_0$.

| Element | $F_2^{SBC}$ | $Z_B'$ | $\epsilon_0$ | $S$ |
|---|---|---|---|---|
| Diamond | 1.47 | −3.2 | 5.8[a] | 1.79 |
| Si | 0.89 | −2.5 | 12.0[b] | 0.52 |
| Ge | 0.82 | −2.6 | 16.0[b] | 0.42 |
| Sn | 0.78 | −2.6 | 24.0[c] | 0.28 |

[a] H. R. Phillip and E. A. Taft, Phys. Rev. **136**, A1445 (1964).
[b] Reference 47.
[c] R. E. Lindquist and A. W. Ewald, Phys. Rev. **135**, A191 (1964).

[72] B. Szigetti, Proc. Phys. Soc. (London) **A204**, 51 (1950).

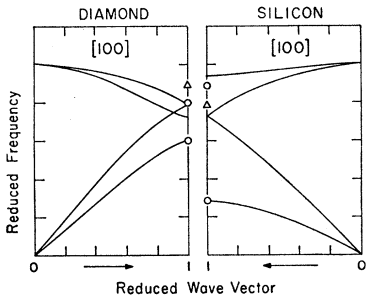


FIG. 10. Comparison of the dispersion curves normalized to the Raman frequency $\omega_0$ along the [100] direction in diamond and Si. The solid lines are the results of the SBC model fitted to $\omega_0$ and $\omega_{TA}(X)$. The points are the experimental values at the zone boundary (Refs. 15 and 20); the circles denote transverse and the triangles, longitudinal, modes.

The most important trend among the SBC parameters in Table V is that $S$ decreases more rapidly than does $F_2^{SBC}$ in going down the table. The major trends in the dispersion curves as one goes from diamond to Sn are explained by the changes in the ratio of $S$ to $F_2^{SBC}$. As an example, Fig. 10 shows the results of the SBC calculations for diamond and Si. The frequencies are normalized to the respective Raman frequencies, and only the [100] direction is considered. The low TA mode in Si is now interpreted as a manifestation of the smallness of the bond charge, i.e., the dielectric constant is large and the Coulombic forces are diminished relative to the non-Coulombic forces. In diamond, the screening is not so good, the bond-charge magnitude is larger, and the TA modes at $X$ are much higher relative to the Raman frequency than is the case in Si. Precisely the same forces explain the fact that the TO modes are generally above the LO modes in Si, whereas the opposite is the case in diamond. The Coulombic forces are further diminished in Ge and grey Sn, explaining the trends in their dispersion curves[18,19] compared to Si.

Let us compare the parameters of the SBC model with those of the detailed calculation for Si. The charge parameter $Z_B'$ as shown in Table V is always greater than the value $Z_B=-2$ predicted above. The difference can be largely attributed to the contribution of longer-range non-Coulombic forces which were omitted in the SBC model, and which would reduce the value of $Z_B'$ needed to fit $\omega_{TA}(X)$. Thus, the major deviations from homology among the dispersion curves are accounted for quite simply in the bond-charge model with the charge parameter $S$ varying roughly, as was predicted by Phillips.[10] Comparing Tables II and V, we see that the values of $F_2(r)$ for Si differ by only 10%, and using (8.5) we find $F_1^{SBC}$ is greater than the calculated $F_1(r)$ by about 30%.

The primary failure of the SBC model is for the elastic constants. Using the parameters given in Table V, the predicted elastic constants $C_{11}$, $C_{44}$, and $C_{11}$–$C_{12}$ are in every case lower than the experimental values. The shear elastic constant $C_{11}$–$C_{12}$ is of particular note;

the formula (8.6g) predicts a value of $C_{11}$–$C_{12}$ which is much too low (by a factor of 2.9 in diamond, 5.7 in Si, and 6.4 in Ge).

The SBC model explains Rosenstock's[73] observation on the experimental vibration frequencies of Si. Rosenstock showed that if all forces between atoms on the same sublattice, e.g., second neighbors in the diamond lattice, are "classical electrostatic" forces, then the sum over all modes of the frequencies squared is independent of wave vector

$$\sum_{\lambda=1}^{3n} \omega_\lambda^2(\mathbf{q}) = \text{const.} \tag{8.8}$$

In the case of Si, Rosenstock showed that (8.8) is obeyed to within the experimental error ($\sim 3\%$). The Coulomb forces in the bond-charge model obey classical electrostatic criteria, and thus the SBC model obeys (8.8) exactly. The small non-Coulombic forces between more distant neighbors in the actual calculations for Si change this conclusion very little; for all calculations described in Sec. VI, the sum rule (8.8) is obeyed to within 5%. Note that the second-neighbor non-Coulombic forces may not be so small in diamond, which can explain the deviations from (8.8) found in that case.[73]

## IX. CONCLUSIONS

The bond-charge model of the electronic response to the displacement of the ions has been shown to lead to phonon dispersion curves for Si in reasonable agreement with experiment. The small transfer of charge into the bonds (total bond charge $2/\epsilon_0 = \frac{1}{6}$ electron) yields qualitative improvements over the free-electron screening model (compare Figs. 1 and 6). In particular, in contrast to the FE model, the noncentral forces in the bond-charge model lead to the result that Si is stable against shear in the diamond structure. In the bond-charge calculation described here, there was one parameter, the curvature of $\epsilon_{\text{eff}}(k)$ at $k=0$, which was used to fit the $C_{11}$ elastic constant. The adjustment affected only the longitudinal acoustic modes within the BZ. All other dispersion curves (in particular, all shear modes) were calculated with no adjustable parameters, using a pseudopotential and an effective dielectric function derived independently.

The agreement with experiment is generally of the order of 10% with larger deviations for the lower frequencies—the worst deviation being 36% for $\omega_{TA}(X)$. All the major features of the dispersion curves are found in the bond-charge calculation. However, there are several detailed features of the dispersion curves which are not found: the LO-TO crossing the [100] direction, the form of the maxima and the minima in the [110] direction, and the characteristic flattening of the TA modes. We have noted that the last-mentioned feature may arise from neglect of the wave-number dependence of the bond-charge form factor.

The conclusions about the phonon dispersion curves computed in both the FE and bond-charge models were shown to be relatively insensitive to the detailed choice of the pseudopotential form factor or effective dielectric function. Only the elastic constants, and to a lesser extent $\omega_{TA}$ at the zone boundaries, were very sensitive to small changes in these functions.

The primary conclusions from the calculations can be stated within the context of the SBC model introduced in Sec. VIII. The SBC model encompasses most of the information derived from the pseudopotential calculation for Si, and makes possible immediate application to all diamond-structure crystals. All essential trends in the dispersion curves among the diamond structure elements were shown to be described by varying the ratio of the Coulombic to the non-Coulombic forces, each of which is described by one parameter in the SBC model. The contribution of the Coulomb forces to the frequencies was found to vary approximately as $1/\epsilon_0$ in agreement with the prediction of Phillips[10] for the magnitude of the bond charge. Within the SBC model was found a relation [Eq. (8.7)] between the bulk modulus and the Raman frequency which was first derived by Szigetti[72] for ionic crystals. Testing this relation for the diamond-structure crystals showed it to be very accurately satisfied in diamond, but less so in Si and Ge, as shown in Table IV. In addition, the observation of Rosenstock[73] on the experimental frequencies of Si was explained by this model.

## ACKNOWLEDGMENTS

The author is grateful to Dr. M. H. Cohen, who suggested this problem and provided guidance throughout the course of this work, and to Dr. J. C. Phillips for many helpful discussions. This work has also benefitted from the author's discussions with Dr. R. M. Pick, Dr. A. K. Rajagopal, Dr. H. L. McMurray, and Dr. A. W. Solbrig, Jr. Thanks are due to Dr. D. L. Price for communicating his data prior to publication.

[73] H. B. Rosenstock, Phys. Rev. **129**, 1959 (1963); **145**, 546 (1966); in *Lattice Dynamics*, edited by R. F. Wallis (Pergamon Press, Ltd., Oxford, 1965), p. 205. As is given correctly in the latter papers, but contrary to the first, the experimental deviations from (8.8) are consistent with a central second-neighbor non-Coulombic force.